



## Article

# Copper, Zinc, and Lead Recovery from Jarosite Pb–Ag Tailings Waste (Part 2)

Vesna Conić \*, Miloš Janošević, Dragana S. Božić, Ljiljana Avramović , Ivana Jovanović , Dejan M. Bugarin and Stefan Đorđević

Mining and Metallurgy Institute Bor, Zelene Bulevar 35, 19210 Bor, Serbia; milos.janosevic@irmbor.co.rs (M.J.); dragana.bozic@irmbor.co.rs (D.S.B.); ljiljana.avramovic@irmbor.co.rs (Lj.A.); ivana.jovanovic@irmbor.co.rs (I.J.); dejan.bugarin@irmbor.co.rs (D.M.B.); stefan.djordjevic@irmbor.co.rs (S.Đ.)

\* Correspondence: vesna.conic@irmbor.co.rs; Tel.: +381-61-1618-224

**Abstract:** The present paper describes the technological solution for obtaining Cu, Zn, Pb, and Ag from jarosite waste raw material, with its simultaneous separation from In and Fe. By roasting at low temperatures, iron was transformed from the  $\text{Fe}_2(\text{SO}_4)_3$  form into  $\text{Fe}_2\text{O}_3$ , which is insoluble in water and slightly soluble in acid. Copper sulfate and zinc sulfate are present in jarosite as sulfates. During temperature roasting, the copper and zinc were still in the form of  $\text{CuSO}_4$  and  $\text{ZnSO}_4$ , i.e., they were easily dissolved in water. This procedure led to good selectivity of Cu and Zn compared to Fe. After water leaching,  $\text{PbSO}_4$  and  $\text{Ag}_2\text{SO}_4$  remained in the solid residue. By treating jarosite with a content of 0.7% Cu, 5.39% Zn, and 5.68% Pb, products of commercial quality were obtained. By roasting jarosite in an electric furnace and leaching the roasted sample in water, leaching degrees of 91.07%, 91.97%, and 9.60% were obtained for Cu, Zn, and Fe, respectively. Using 1 M NaOH in the leaching solution, 99.93% Fe was precipitated to pH = 4. Cu in the form of  $\text{CuSO}_4$  was further treated by cementation with Zn, after which cement copper was obtained as a commercial product. Zn in the form of  $\text{ZnSO}_4$  was further treated by precipitation with  $\text{Na}_2\text{CO}_3$  to obtain  $\text{ZnCO}_3$  concentrate of commercial grade. The total recovery of Pb and Ag, which were treated by chloride leaching, was 96.05% and 87.5%, respectively. The resulting  $\text{NaPbCl}_3$  solution was further treated with  $\text{Na}_2\text{CO}_3$  solution, whereby  $\text{PbCO}_3$  was obtained as a commercial product. The produced  $\text{PbCO}_3$  could be further subjected to roasting to obtain soluble PbO. In these investigations,  $\text{PbCO}_3$  was smelted where a Pb anode was obtained; this was electrolytically refined to a Pb cathode. The proposed process does not pollute the environment with As and Cd.

**Keywords:** jarosite processing; hydrometallurgy; low-temperature roasting; water leaching; metal recovery



**Citation:** Conić, V.; Janošević, M.; Božić, D.S.; Avramović, L.; Jovanović, I.; Bugarin, D.M.; Đorđević, S. Copper, Zinc, and Lead Recovery from Jarosite Pb–Ag Tailings Waste (Part 2). *Minerals* **2024**, *14*, 791. <https://doi.org/10.3390/min14080791>

Academic Editor: Ilhwan Park

Received: 19 June 2024  
Revised: 12 July 2024  
Accepted: 16 July 2024  
Published: 31 July 2024



**Copyright:** © 2024 by the authors. Licensee MDPI, Basel, Switzerland. This article is an open access article distributed under the terms and conditions of the Creative Commons Attribution (CC BY) license (<https://creativecommons.org/licenses/by/4.0/>).

## 1. Introduction

The demand for increasing metal production and decreasing grades of primary mineral deposits has led researchers to seek alternative methods of pyrometallurgical processing. There has been an increasing share of hydroprocessing plants for secondary raw material treatment since the 1990s [1]. One of these secondary raw materials is jarosite which, in its precipitation process, loses significant amounts of copper, zinc, lead, and silver [2]. The first three are widely used in various branches of the industry. Lead and zinc play important roles in human lives and are widely used in lead–acid batteries, galvanization, rolled and extruded products, alloys, pigments, brass and bronze, and chemicals [3–5]. Erdem et al. [6] and Turan et al. [7] conducted important studies on jarosite (zinc plant residue) as a raw material, with the main goal being the recovery of Pb and Zn from jarosite. The demand for lead and zinc increases every year, and by 2050, it will be measured in millions of tons [8]. New lead–zinc deposits have not been discovered in recent years, and exploring the new sources of these metals will be a challenge. Considering that primary ore deposits have been exhausted, secondary raw materials have been gaining

increasing importance. The uncertainty surrounding the behavior of jarosite waste has spurred the implementation of metallurgical procedures. Lead is a toxic metal and is discharged as a by-product from different types of industries [9–11]. The presence of lead in water resources can cause diseases such as hepatitis and anemia [12–15]. Researchers have proposed diverse methodologies for recovering valuable minerals from these wastes. Where pyrometallurgical treatment was the primary treatment of such kinds of waste in the past, ecological hydro- and biotechnological procedures are now being increasingly applied. The advantages of the hydrometallurgical technique include high metal recovery, higher tolerance towards impurities, modularity, flexibility, lower energy consumption, and lower capital and operative costs. Several attempts have been made to decompose jarosites using sulfuric acid, hydrochloric acid with the addition of calcium chloride, ammonia, and sodium or calcium hydroxides [16–19]. Obtaining metal from waste of any kind, solid or liquid, is of great importance [20,21]. Obtaining useful metals from waste can be more energy efficient, economical, and ecological. The opening of new mines requires large investment (connection to infrastructure, excavation, transport, etc.), and, considering that the reserves of useful metals have been depleted in existing mines (low concentrations of metals in the ore) and that their exploitation is unprofitable, the world is increasingly tending to use available resources, such as tailings and other waste.

Various studies have been conducted on the treatment of jarosite, including the following: the co-precipitation of copper and zinc with lead jarosite [22]; the cyanidation of argentian potassium jarosite in alkaline media [23]; sodium arsenojarosite decomposition in alkaline media [24]; the release of arsenic and antimony in alunite–jarosite and beudantite group minerals [25]; the alkaline decomposition of ammonium–sodium jarosite with arsenic [26]; and the thermal decomposition of jarosites with potassium, sodium, and lead [27].

Considering that waste contains harmful and useful metals, and because it is important to add value to useful metals, a new, environmentally acceptable method for the extraction of these useful metals should be proposed.

Our initial studies were focused on the application of different types and conditions of leaching [28], where, in addition to the metals Cu, Zn, and In, more than 80% of Fe was leached. For this reason, further experiments were carried out to convert Fe into insoluble hematite through roasting and water leaching, and to selectively extract Cu, Zn, and In in this way. The roasting and leaching conditions, with selected parameters, are presented in the paper “Indium Recovery from Jarosite Pb–Ag Tailings Waste Part 1” [29].

The roasting of jarosite was conducted at three different temperatures: 530 °C, 570 °C, and 630 °C. The results show that almost all the iron was transformed into hematite in the sample fired at 630 °C, whereas in the samples fired at 530 °C and 570 °C, part of the iron remained in the form of magnetite. Subsequent leaching of the precipitates revealed that the greatest leaching of useful metals was achieved by leaching the precipitates obtained at 530 °C. Copper sulfate and zinc sulfate are present in jarosite as sulfates. They decomposed at 600 °C and 740 °C, respectively. For this reason, at the selected drying temperature, they remained in the form of sulfates that are easily leached in water.

Jarosite Pb–Ag sludge was formed at the Elixir Zorka factory in Šabac, Serbia, and is a valuable residue obtained by leaching with hot acid.

This work represents significant technical support for the valorization of Cu, Zn, Pb, and Ag from jarosite waste and for obtaining products (cement Cu, ZnCO<sub>3</sub>, PbCO<sub>3</sub>, and Pb) of commercial quality.

## 2. Materials and Methods

### *Analytical Determinations*

The acidity of the leach solution was measured using a combined pH electrode Aqua Lytic SD300, produced in Germany. The concentration of zinc, copper, iron, lead, and silver in solution was measured using absorption spectrometry (Perkin-Elmer 403) with a

spectrometer produced in the USA. An optical laser particle size analyzer (MASTERSIZER 2000, Hydro2000MU, UK) was used to determine the particle size distribution of the products.

XRD analysis was performed using a “PHILIPS” X-ray diffractometer (Netherlands, model PW-1710/1820, with a curved graphite monochromator and a scintillation counter. The intensities of diffracted  $\text{CuK}\alpha$  X-ray radiation ( $\lambda = 1.54178 \text{ \AA}$ ) were measured at room temperature in intervals of  $0.02^\circ$  ( $2\theta$ ), with a time of 1 s, over a range from  $4$  to  $65^\circ$  ( $2\theta$ ).

Electron microscopy method: The sample was coated with gold (20 nm layer, density  $2.25 \text{ g/cm}^3$ ). The textual part was accompanied by electron micrographs and SEM chemical spectra. SEM model: JEOL JSM-7001F—Magnification X 5–1,000,000 (Japan).

The reduction melting of  $\text{PbCO}_3$  was performed in the electric furnace by FIOA, Italy.

### 3. Results and Discussion

#### 3.1. Chemical and Mineralogical Analysis of Jarosite

Homogenization was performed and a representative sample was sent for chemical and mineralogical analysis. The chemical analysis of the sample is shown in Table 1.

**Table 1.** Chemical analysis of the Pb–Ag jarosite sample.

| Element | Cu<br>% | Zn<br>% | Fe<br>% | Ag<br>% | Pb<br>% | In<br>% | S<br>% | N <sub>2</sub><br>% | H <sub>2</sub><br>% | C<br>% |
|---------|---------|---------|---------|---------|---------|---------|--------|---------------------|---------------------|--------|
| Content | 0.7     | 5.39    | 30.61   | 0.034   | 5.68    | 0.0343  | 9.61   | 1.315               | 1.670               | 0.126  |

The diffractogram obtained from the XRD analysis of the jarosite waste sample is shown in [29]. The presented minerals are jarosite in the form of  $\text{NH}_4\text{Fe}_3(\text{SO}_4)_2(\text{OH})_6$ , magnetite in the form of  $\text{Fe}_3\text{O}_4$ , and anglesite in the form of  $\text{PbSO}_4$ .

There is a possibility that Zn is in the jarosite structure. The detection limit is about 1%. Jarosite and magnetite raise the baseline of the diffractogram because they contain a large proportion of Fe, which creates secondary fluorescent radiation that is scattered everywhere. As a result, the detection limit is higher than 3–5%, meaning that crystalline phases containing Zn may be below the detection threshold.

There is a possibility that zinc is present in the form of an amorphous substance that cannot be detected.

Magnetite belongs to the spinel group, so the presence of other minerals from the spinel group that have peaks that coincide with magnetite is also possible. Therefore, there is a possibility that zinc minerals in the sample may be present in the form of zinc-ferrite, franklinite, and granite.

#### 3.2. Roasting and Leaching of Jarosite Pb–Ag Deposits

Detailed laboratory tests of the combined process, which includes roasting the jarosite Pb–Ag sample and leaching the resulting product (calcine), were performed. The results are presented in [29]. The accepted treatment parameters for Pb–Ag jarosite sample include roasting for 4 h at a temperature of  $530^\circ\text{C}$  and leaching of the calcine with water at a solid–liquid phase ratio of 1:5 for 1 h, during which high leaching of the examined metals and low iron leaching obtained Cu and Zn. The conditions of the combined process and the obtained results of percentage metal leaching are shown in Table 2.

**Table 2.** Conditions for the jarosite roasting and leaching process.

| Roasting Time 4 h  |                                 | Leaching with H <sub>2</sub> O<br>(Solid–Liquid = 1:5),<br>t = 1 h and pH after Leaching |         | Recovery |         |      |
|--------------------|---------------------------------|--|---------|----------|---------|------|
| Sample Mass<br>(g) | Roasting<br>Temperature<br>(°C) | pH   | Cu<br>% | Zn<br>%  | Fe<br>% |      |
| 1.                 | 100                             | 530  | 2.25    | 91.07    | 91.97   | 9.60 |

From Table 2, it can be seen that under the applied conditions of roasting and leaching, the recovery amounts of Cu, Zn, and Fe were 91.07%, 91.97%, and 9.6%, respectively. It can also be observed from the results that after the roasting of jarosite and the leaching of the calcine in water, the measured pH of the solution was 2.25.

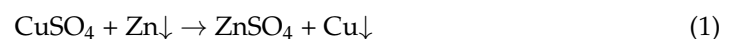
After leaching, Pb and Ag remained in the solid leach residue.

### 3.3. Treatment of Sulfate Solution

A sulfate solution containing Cu, Zn, Fe, and In was treated to separate the metals. During the precipitation phase, the pH level was controlled and maintained at 4 using a concentrated NaOH solution. The detailed procedure is described in [29].

### 3.4. Cementation of Cu from the Solution after the Precipitation of Fe

After precipitation, the macro-components Cu and Zn remained in the solution, which were present in the solution in the form of sulfates, specifically  $\text{CuSO}_4$  and  $\text{ZnSO}_4$ , respectively. To selectively extract copper from the solution, cementation was performed at a pH of 2 with zinc powder, a metal that is more electronegative than copper. The necessary amount of zinc for the cementation process was calculated based on the stoichiometrically required amount with 50% excess. The process of cementation, during which copper is converted into cement slurry, takes place according to reaction (1).



The obtained cement copper was washed, dried, and subjected to chemical analysis. Characterization of the obtained cement copper showed that the metal content in it was as follows: Cu = 75.97%, Zn = 7.31%, Fe = 0.005%, In < 0.095%, S = 1.9%, Ga < 0.002%, Ge < 0.002%, Ag = 0.042%, and Pb = 0.06%.

In the leaching phase, copper was not completely leached but was recovered at 91.07%, which means that the loss in this phase was 8.93%.

Copper losses occurred during indium precipitation and copper cementation, amounting to 11.3%. During the precipitation process, approximately two-thirds of the total 11.3% of Cu remained trapped (occluded) in the precipitate and the remaining one-third of the total 11.3% was not fully cemented because the cementation process was never completed.

The product Cem Cu was offered to the Zijin Copper Bor Srbija smelter. The limiting factors for product quality were as follows: 3% moisture content, up to 5% Pb, up to 8% Zn, and granulometric composition for treatment in the smelter.

The offered product was accepted by the company for further processing and to obtain cathodic copper.

#### 3.4.1. Granulometric Analysis of Cement Copper

A granulometric analysis of cement copper was performed, and the results are shown in Figure 1.

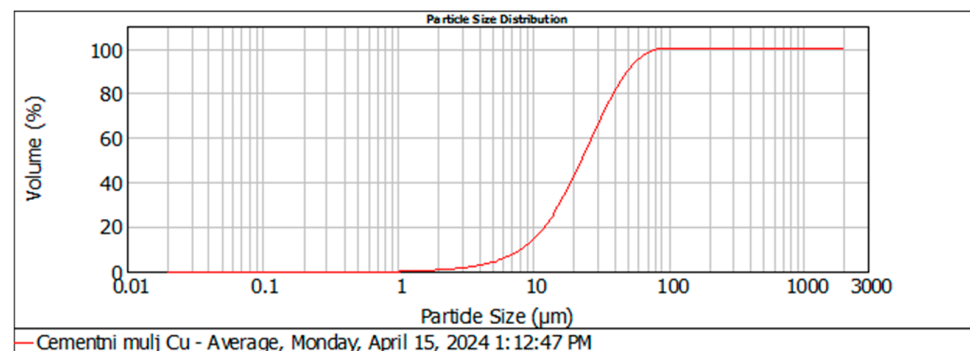


**Figure 1.** Graphic representation of the content of the identified size classes and the granulometric sample composition of Cem Cu, showing the average undersize distribution curve values.



From the results of the granulometric composition of the sample, it can be observed that the size class of 50.258  $\mu\text{m}$  is represented by 90%, the size class of 23.019  $\mu\text{m}$  is represented by 50%, and the size class of 8.157  $\mu\text{m}$  is represented by 10%.

### 3.4.2. SEM-EDS Analysis of Cement Copper

The diffractogram of Cu cement samples is shown in Figure 2. Copper (Cu) and cuprite ( $\text{Cu}_2\text{O}$ ) crystalline phases were identified in the Cu cement sample. Copper is more present in the sample than cuprite.

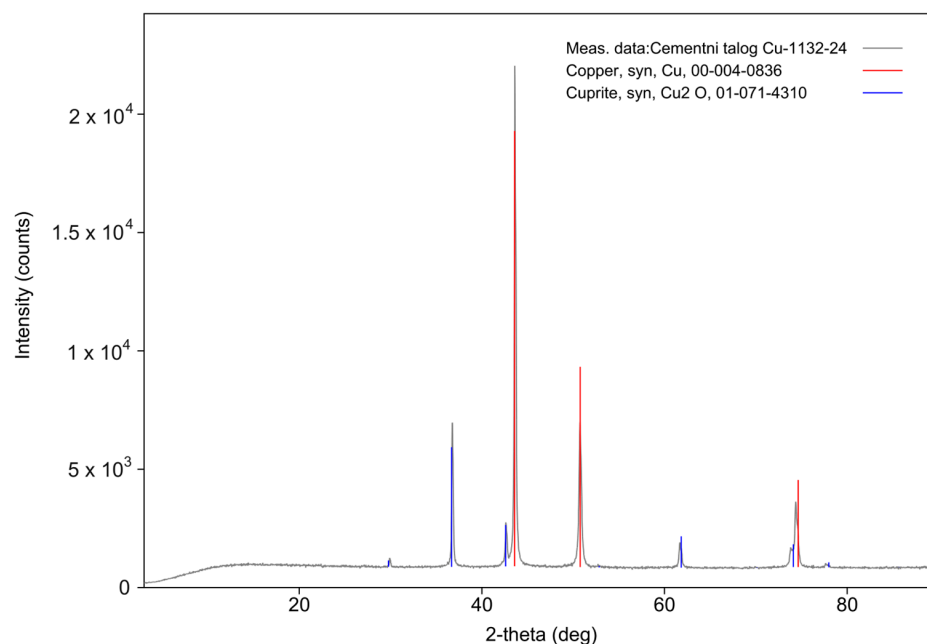


**Figure 2.** Diffractogram of cement copper.

The presence of the elemental copper crystalline phase was determined in the analyzed sample. The sample was very homogeneous. The elemental copper content was much more present, whereas the rest was copper oxide. Photomicrographs of the tested sample are shown in Figure 3.

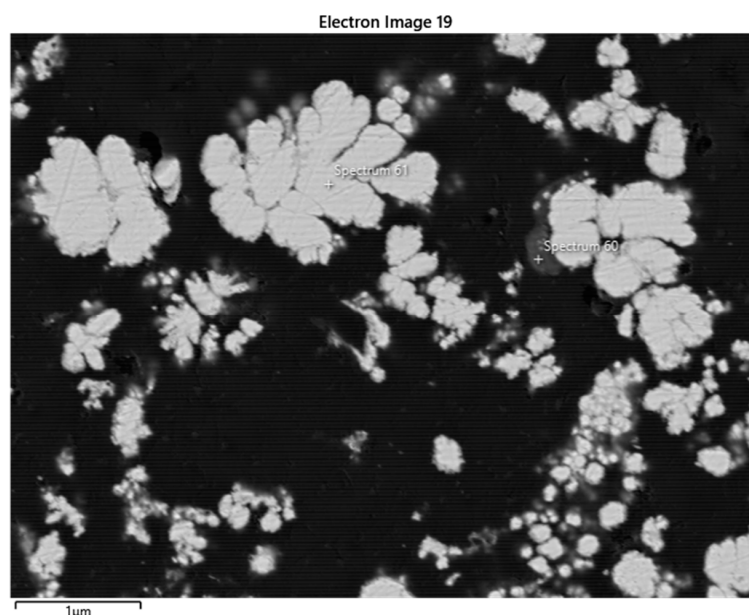


**Figure 3.** Photomicrograph of elemental copper in the “Cu cement” sample.

Figure 4 shows the chemical spectrum of spectrum 61, which was mapped using photomicrograph 3.

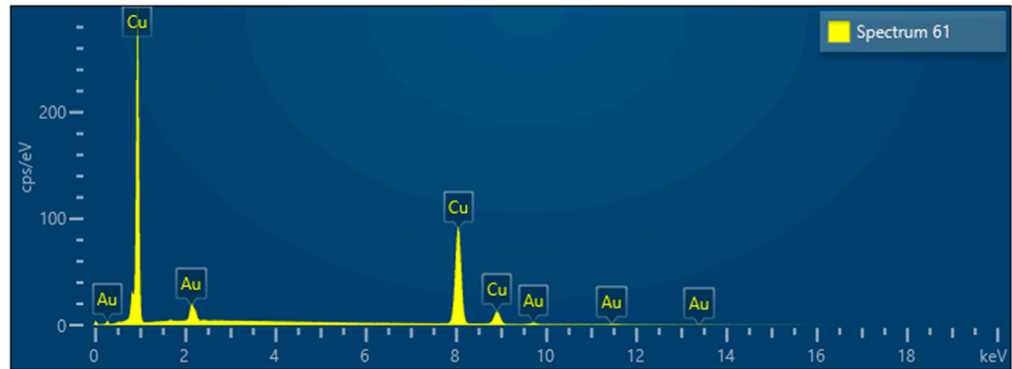


Figure 4. Chemical spectrum from Figure 3 (spectrum 61).

Table 3 presents the results of the chemical analysis of the summary spectrum of the cement copper sample.

Table 3. Chemical composition from Figure 4 (spectrum 61).

| Spectrum 61 |           |          |                |
|-------------|-----------|----------|----------------|
| Element     | Line Type | Weight % | Weight % Sigma |
| Cu          | K series  | 100.00   | 0.00           |
| Total       |           | 100.00   |                |

Figure 5 presents the mapping of the entire surface of the sample, highlighting the distribution of the copper element.

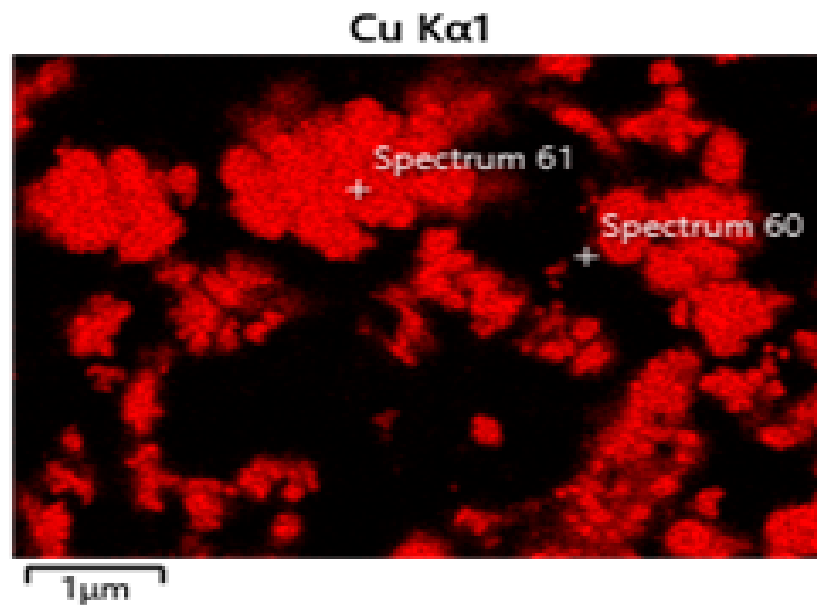
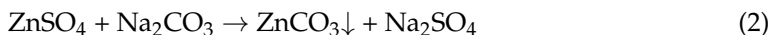


Figure 5. Copper mapping image. Mapping of the copper element from Figure 3.

### 3.5. Precipitation of ZnCO<sub>3</sub> from the Solution after the Cementation of Cu

After copper cementation, the solution was filtered and prepared to obtain ZnCO<sub>3</sub> from ZnSO<sub>4</sub>. The pH value of the solution after Cu cementation was measured as 2.84. The

precipitation of Zn as ZnCO<sub>3</sub> was achieved by adding 10% Na<sub>2</sub>CO<sub>3</sub> solution until the pH reached 8. The precipitation process of Zn as ZnCO<sub>3</sub> occurs according to reaction (2).



The resulting zinc carbonate was washed, dried, and subjected to chemical analysis. Characterization of the obtained zinc carbonate showed the following composition: Zn = 52.22%, Cu = 0.26%, Fe = 0.84%, Pb = 0.002%, Ag < 0.001%, S = 2.24%, and In < 0.002%.

The obtained ZnCO<sub>3</sub> product, along with the presented analysis, was offered to KCM Bulgaria Company. The company itself analyzed the product and determined that the content of As and Cd metals was <0.001% and 0.14%, respectively, and that the quality of the product met their needs. The offered product was accepted by the company for further processing and to obtain cathodic zinc.

### 3.5.1. Granulometric Analysis of ZnCO<sub>3</sub>

A granulometric analysis of zinc carbonate was performed, and the results are shown in Figure 6.

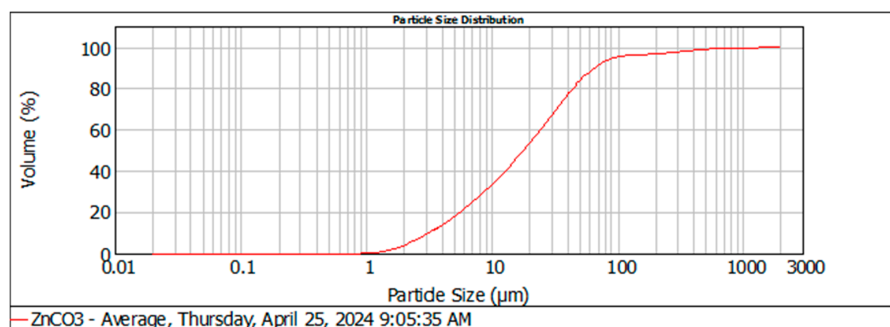


Figure 6. Graphic representation of the content of the identified size classes and the granulometric sample composition of ZnCO<sub>3</sub>, showing the average undersize distribution curve values.

From the results of the granulometric composition of the sample, it can be observed that the size class of 65.035 µm is represented by 90%, the size class of 18.052 µm is represented by 50%, and the size class of 3.214 µm is represented by 10%.

### 3.5.2. SEM-EDS Analysis of ZnCO<sub>3</sub>

The diffractogram of the following crystalline phases was determined in the analyzed sample and is presented in Figure 7, including ZnCO<sub>3</sub>, ZnO, Zn<sub>5</sub>(CO<sub>3</sub>)<sub>2</sub>(OH)<sub>6</sub>, and CaCO<sub>3</sub>.

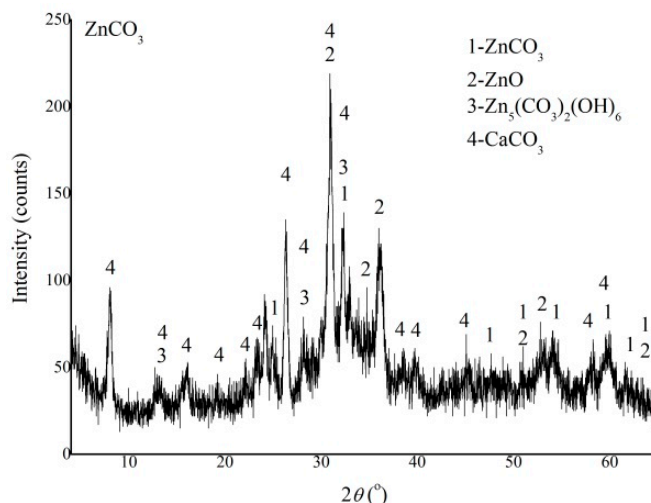


Figure 7. Diffractogram of the ZnCO<sub>3</sub> sample.

A photomicrograph of the tested sample is shown in Figure 8.

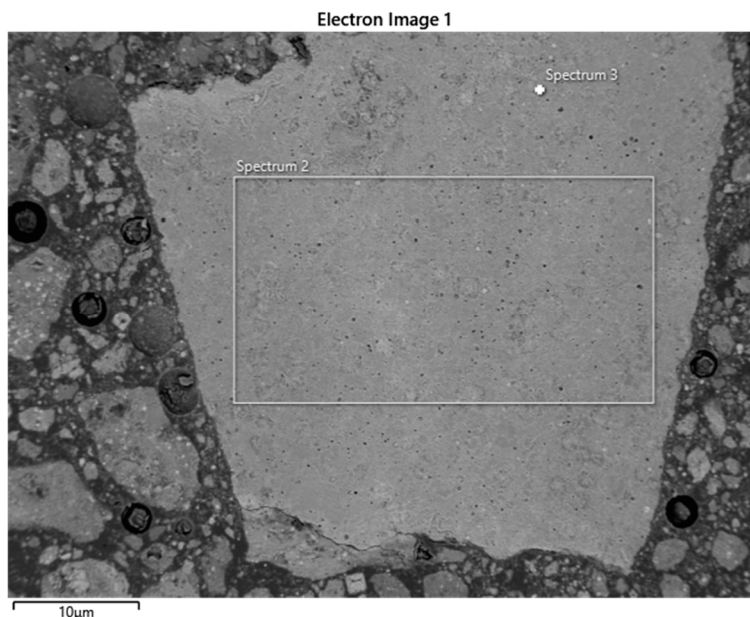


Figure 8. Photomicrograph of the ZnCO<sub>3</sub> phase.

Figure 9 shows the chemical spectrum of spectrum 3, which was mapped using photomicrograph 8 of the analyzed sample.

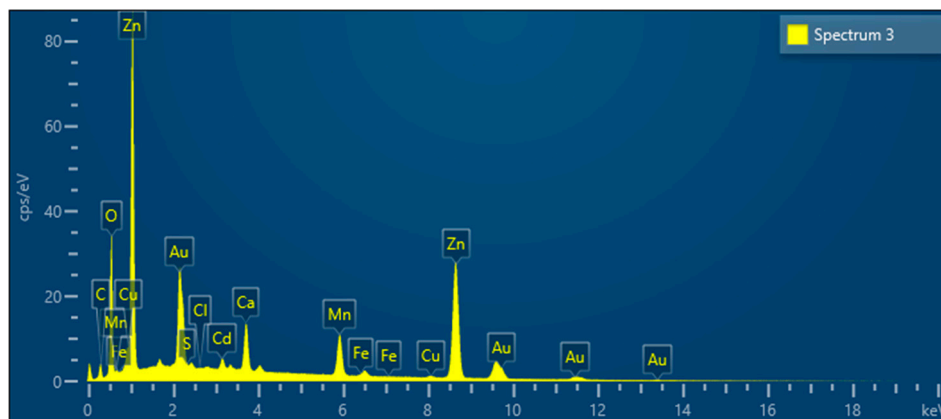


Figure 9. Chemical spectrum from Figure 8 (spectrum 3).

Table 4 shows the results of the chemical analysis of the spectrum of the zinc carbonate sample.

Table 4. Chemical composition from Figure 9 (spectrum 3).

| Spectrum 3 |           |          |                |
|------------|-----------|----------|----------------|
| Element    | Line Type | Weight % | Weight % Sigma |
| C          | K series  | 15.73    | 0.67           |
| O          | K series  | 29.15    | 0.28           |
| S          | K series  | 0.07     | 0.03           |
| Cl         | K series  | 0.02     | 0.02           |
| Ca         | K series  | 2.92     | 0.04           |
| Mn         | K series  | 5.37     | 0.07           |

Table 4. Cont.

| Spectrum 3 |           |          |                |
|------------|-----------|----------|----------------|
| Element    | Line Type | Weight % | Weight % Sigma |
| Fe         | K series  | 0.05     | 0.03           |
| Cu         | K series  | 0.51     | 0.05           |
| Zn         | K series  | 44.66    | 0.39           |
| Cd         | L series  | 1.52     | 0.06           |
| Total      |           | 100.00   |                |

### 3.6. Characterization of the Solution after the Precipitation of ZnCO<sub>3</sub>

The characterization of wastewater after ZnCO<sub>3</sub> precipitation is shown in Table 5.

Table 5. Characterization of wastewater after ZnCO<sub>3</sub> precipitation.

| Parameter   | Unit of Measure | Test Result | Emission Limit Value |
|---|-----------------|-------------|----------------------|
| pH  |                 | 8.0         | 6.5–9.5              |
| Chemical consumption of oxygen  | mg/L            | 7.34        | 1000                 |
| Biochemical consumption of oxygen   | mg/L            | 24          | 500                  |
| Total inorganic nitrogen N (NH <sub>3</sub> -N, NO <sub>3</sub> -N, NO <sub>2</sub> -N) | mg/L            | 1.15        | 120                  |
| Total nitrogen, N   | mg/L            | 1.472       | 150                  |
| Ammonia, NH <sub>4</sub> -N   | mg/L            | 0.37        | 100                  |
| Precipitable substances after 10 min  | mg/L            | <0.2        | 150                  |
| Phosphorus, P   | mg/L            | <0.03       | 20                   |
| Extract with organic solvents   | mg/L            | <0.05       | 50                   |
| Mineral oils  | mg/L            | <0.05       | 30                   |
| Total salts   | mg/L            | 142         | 5000                 |
| Phenols   | mg/L            | <0.1        | 50                   |
| Sulfates, SO <sub>4</sub> <sup>2-</sup>   | mg/L            | 83.7        | 400                  |
| Chlorides, Cl <sup>-</sup>  | mg/L            | 9.47        | 30                   |
| Fluorides, F <sup>-</sup>   | mg/L            | 1.30        | 50                   |
| Sulfides, S <sup>2-</sup>   | mg/L            | <0.005      | 5                    |
| Arsenic, As   | mg/L            | <0.02       | 0.2                  |
| Copper, Cu  | mg/L            | 0.009       | 2                    |
| Barium, Ba  | mg/L            | <0.009      | 0.5                  |
| Zinc, Zn  | mg/L            | 0.196       | 2                    |
| Iron, Fe  | mg/L            | <0.007      | 200                  |
| Chrome, Cr  | mg/L            | <0.005      | 1                    |
| Chrome, Cr <sup>6+</sup>  | mg/L            | <0.005      | 0.5                  |
| Cadmium, Cd   | mg/L            | 0.045       | 0.1                  |
| Tin, Sn   | mg/L            | <0.05       | 2                    |
| Cobalt, Co  | mg/L            | 0.062       | 1                    |
| Manganese, Mn   | mg/L            | 0.006       | 5                    |
| Molybdenum, Mo  | mg/L            | <0.007      | 0.5                  |
| Nickel, Ni  | mg/L            | 0.037       | 1                    |



Table 5. Cont.

| Parameter   | Unit of Measure | Test Result | Emission Limit Value |
|-------------|-----------------|-------------|----------------------|
| Lead, Pb    | mg/L            | <0.02       | 0.2                  |
| Silver, Ag  | mg/L            | <0.005      | 0.2                  |
| Mercury, Hg | mg/L            | <0.0005     | 0.05                 |

Based on the results shown in Table 5, it can be concluded that the emission limit values of polluting substances in the technological wastewater, before their discharge into the public sewage system, meet the limit values.

The resulting wastewater can be returned to the process as technical return water and used for leaching the calcine.

### 3.7. Chloride Leaching of the Solid Residue with NaCl

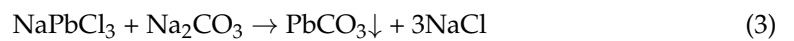
After calcine leaching in water, a solid residue containing PbSO<sub>4</sub> was subjected to chloride leaching in NaCl in order to leach Pb. The leaching conditions were as follows: a salt concentration of 250 g/L NaCl, a solid–liquid phase ratio of 1:20, a temperature of 80 °C, and a leaching time of 20 min. These conditions were determined in our earlier research when polymetallic raw material was leached [30]. The results of metal leaching are shown in Table 6.

Table 6. Percentage of metal recovery in the process of chloride leaching of the solid residue.

| Metal Recovery | Pb %  | Ag %  | Fe % | Cu % | Zn % |
|----------------|-------|-------|------|------|------|
|                | 96.05 | 87.50 | 0.02 | 6.22 | 7.51 |

After chloride leaching, a solution of NaPbCl<sub>3</sub> was obtained. The measured pH value of the solution was 6.86. The precipitation of Pb in the form of PbCO<sub>3</sub> was achieved by adding 10% Na<sub>2</sub>CO<sub>3</sub> solution until the pH reached 8.

The precipitation of PbCO<sub>3</sub> takes place according to reaction (3).



Characterization of the obtained lead carbonate showed the following content: Pb = 67.50%, Ag = 0.47%, Cu = 0.55%, Zn = 5.63%, Fe = 0.08%, S = 0.14%, and In < 0.06%.

#### 3.7.1. Granulometric Analysis of PbCO<sub>3</sub>

A granulometric analysis of lead carbonate was performed, and the results are shown in Figure 10.

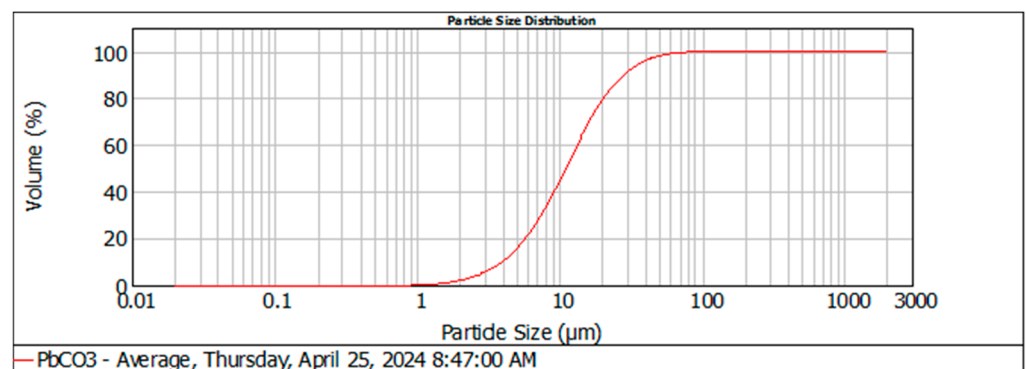
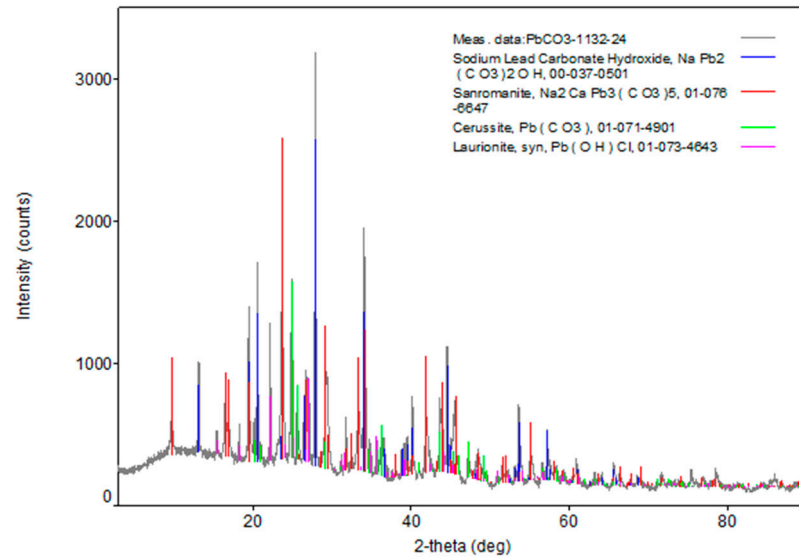


Figure 10. Graphic representation of the content of the identified size classes and the granulometric sample composition of PbCO<sub>3</sub>, showing the average undersize distribution curve values.

From the results of the granulometric composition of the sample, it can be observed that the size class of 28.629  $\mu\text{m}$  is represented by 90%, the size class of 10.976  $\mu\text{m}$  is represented by 50%, and the size class of 3.966  $\mu\text{m}$  is represented by 10%.

### 3.7.2. SEM-EDS Analysis of $\text{PbCO}_3$

The diffractogram of  $\text{PbCO}_3$  samples is shown in Figure 11. In the  $\text{PbCO}_3$  sample, the crystalline phases are sodium–lead–carbonate–hydroxide ( $\text{NaPb}_2(\text{CO}_3)_2\text{OH}$ ), sanromanite ( $\text{Na}_2\text{CaPb}_3(\text{CO}_3)_5$ ), cerussite ( $\text{PbCO}_3$ ), and laurionite ( $\text{Pb}(\text{OH})\text{Cl}$ ). Sodium–lead–carbonate–hydroxide and sanromanite are more abundant in the sample than cerussite and laurionite.



**Figure 11.** Diffractogram of the  $\text{PbCO}_3$  sample.

Photomicrographs of the tested sample are shown in Figure 12.

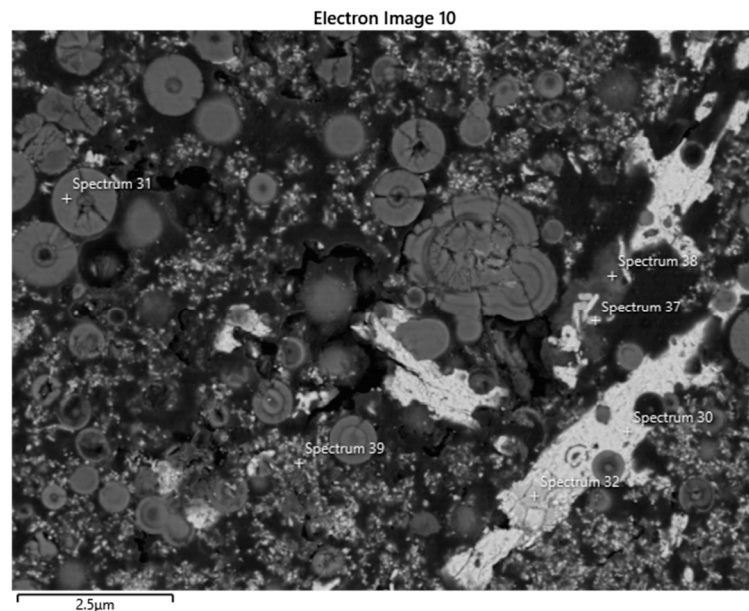


**Figure 12.** Photomicrograph of  $\text{PbCO}_3$ .

Figure 13 shows the chemical spectrum of spectrum 37, which was mapped using photomicrograph 12 of the analyzed sample.

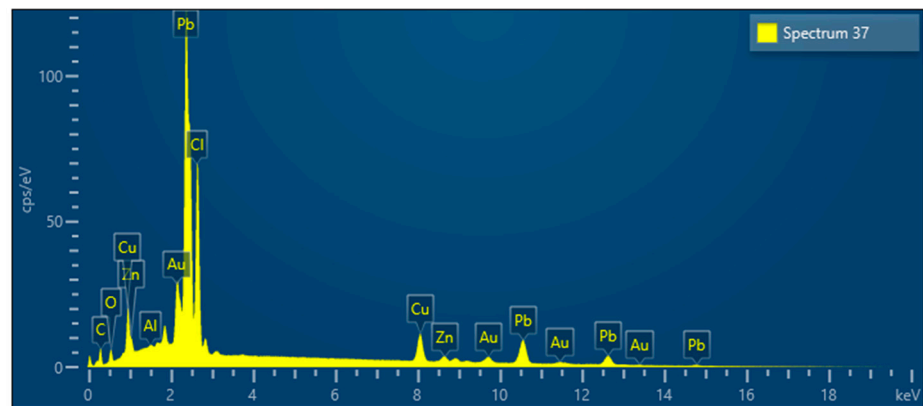


Figure 13. Chemical spectrum from Figure 12 (spectrum 37).

Table 7 shows the results of the chemical analysis of spectrum 37 of the lead carbonate sample.

Table 7. Chemical composition from Figure 13 (spectrum 37).

| Spectrum 37 |           |          |                |
|-------------|-----------|----------|----------------|
| Element     | Line Type | Weight % | Weight % Sigma |
| C           | K series  | 21.32    | 0.39           |
| O           | K series  | 4.45     | 0.12           |
| Al          | K series  | 0.12     | 0.02           |
| Cl          | K series  | 12.07    | 0.09           |
| Cu          | K series  | 8.16     | 0.09           |
| Zn          | K series  | 1.99     | 0.07           |
| Pb          | M series  | 51.89    | 0.29           |
| Total       |           | 100.00   |                |

Figure 14 presents the mapping of the entire surface of the sample, showing the distribution of lead, calcium, and oxygen elements.

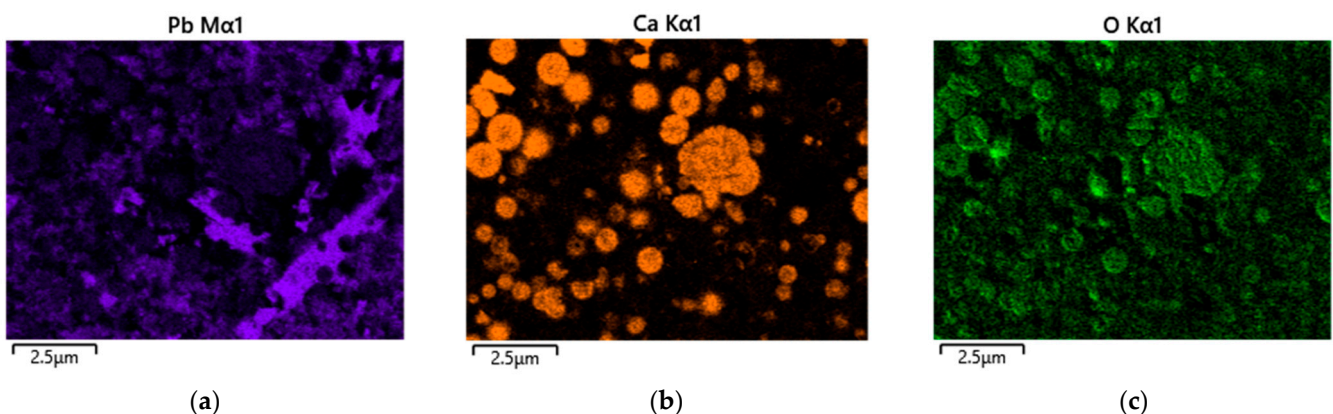


Figure 14. Lead mapping images. (a) Mapping the lead element from Figure 12. (b) Mapping the calcium element from Figure 12. (c) Mapping the oxygen element from Figure 12.

XRD shows the crystalline phase of the product and the form in which it is present. SEM-EDS was performed to unequivocally confirm the presence of  $\text{Cu}_2\text{CO}_3(\text{OH})_2$ ,  $\text{ZnCO}_3$ , and  $\text{PbCO}_3$ . The percentage content on the spectra does not show the metal content in the

analyzed sample; yet, based on the percentage ratios in the spectrum, it indicates the phase ratio and shows the compound.

The copper content in the cement suspension was determined using the electrogravimetric method. The content of Zn in  $ZnCO_3$  and Pb in  $PbCO_3$  was determined by dissolving them and determining the metal content using volumetric titration. Based on the calculations, the metal content in the products was determined. Chemical analysis is a precise quantitative analysis that shows the exact composition of the product.

The appearance of Au in the spectra is due to the steam up of samples using gold during the preparation process for SEM-EDS analysis.

The practical importance of determining the granulometric composition of the obtained products is that it allows the future customer to understand in which part of the production process can be applied, considering that these are commercial products.

### 3.8. Processing of $PbCO_3$

$PbCO_3$  can be roasted at  $550\text{ }^\circ\text{C}$  to obtain  $PbO$ , which can be sold. However, in our investigation,  $PbCO_3$  was melted at  $950\text{ }^\circ\text{C}$  to produce the Pb anode. This Pb anode was further treated through electro-refining to obtain the Pb cathode (Figure 15).

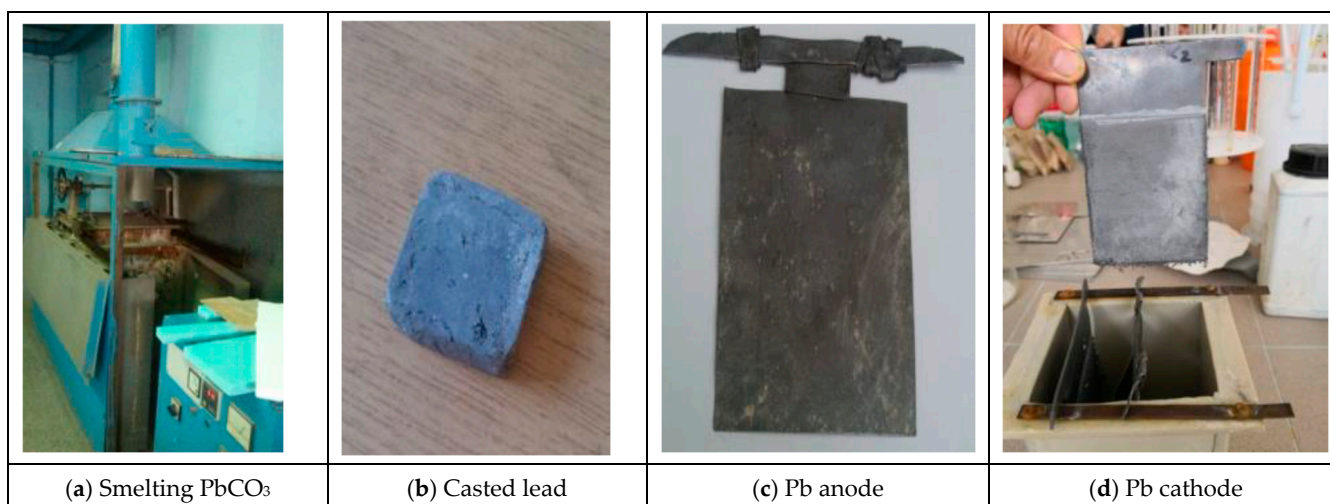


**Figure 15.** Smelting of  $PbCO_3$  and the refinement of Pb: (a) smelting, (b) casting, (c) Pb anode, and (d) Pb cathode.

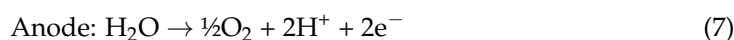
The mixtures for reduction melting were as follows: 81 g of  $PbCO_3$ , 66 g of  $Na_2CO_3$ , 33 g of Borax, and 16 g of carbon. When melting  $PbCO_3$ , the following reactions occur:



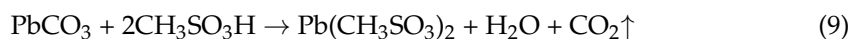
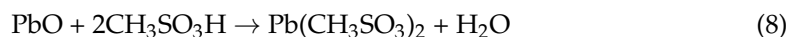
Raw lead (lead anode) was obtained through the reduction smelting of lead oxide. After melting, the raw lead was poured and a seal was made, which was rolled into the anode. The rolled Pb anode was further subjected to electrolytic refining.

#### Electrolytic Refining of the Pb Anode

Cathodic lead is obtained through the electrolysis of raw lead, according to the following reactions:



The electrolyte for electrolytic lead refining is obtained by dissolving lead oxide or lead carbonate in methane-sulfonic acid, according to the following reactions:



The conditions for anode lead refining were as follows: methane-sulfonic acid at 100 g/L, Pb at 200 g/L, organic additive (polyethylene glycol) at 0.25 g/L, a temperature of 20–30 °C, and a Dk of 1.5–3 A/dm<sup>2</sup>.

Commercial-quality lead with 99.95% purity was obtained through the electrolytic refining of lead anodes.

Pb was further used in MMI Bor as a collector during cupellation for the analytical determination of Au and Ag in the samples.

### 3.9. TCLP and LP Test of Solid Residue after Pb and Ag Leaching

After Pb and Ag leaching, the LP test of the solid residue and the TCLP (Toxicity Characteristic Leaching Procedure) test were performed. The solid residue was examined for disposal. The waste was examined using a leachability test and a toxicity test. The results of the LP test are shown in Table 8. The results of the TCLP test are shown in Table 9.

**Table 8.** Results of the chemical test of the solid residue: LP test.

| Parameter                     | Unit       | Found Value | Reference Value for Inert Waste | Reference Value for Non-Hazardous Waste | Reference Value for Hazardous Waste |
|-------------------------------|------------|-------------|---------------------------------|---|-------------------------------------|
| Antimony, Sb                  | mg/kg × dm | <0.11       | 0.06                            | 0.7                                     | 5                                   |
| Arsenic, As                   | mg/kg × dm | <0.2        | 0.5                             | 2                                       | 25                                  |
| Copper, Cu                    | mg/kg × dm | 0.07        | 2                               | 50                                      | 100                                 |
| Barium, Ba                    | mg/kg × dm | 0.13        | 20                              | 100                                     | 300                                 |
| Cadmium, Cd                   | mg/kg × dm | <0.08       | 0.04                            | 1                                       | 5                                   |
| Molybdenum, Mo                | mg/kg × dm | <0.15       | 0.5                             | 10                                      | 30                                  |
| Nickel, Ni                    | mg/kg × dm | <0.07       | 0.4                             | 10                                      | 40                                  |
| Lead, Pb                      | mg/kg × dm | 0.20        | 0.5                             | 10                                      | 50                                  |
| Selenium, Se                  | mg/kg × dm | <0.33       | 0.1                             | 0.5                                     | 7                                   |
| Chrome, Cr                    | mg/kg × dm | <0.05       | 0.5                             | 10                                      | 70                                  |
| Zinc, Zn                      | mg/kg × dm | 0.6         | 4                               | 50                                      | 200                                 |
| Mercury, Hg                   | mg/kg × dm | <0.005      | 0.01                            | 0.2                                     | 2                                   |
| SO <sub>4</sub> <sup>2-</sup> | mg/kg × dm | 900         | 1000                            | 20,000                                  | 50,000                              |
| Cl <sup>-</sup>               | mg/kg × dm | 120         | 800                             | 15,000                                  | 25,000                              |
| F <sup>-</sup>                | mg/kg × dm | <8          | 10                              | 150                                     | 500                                 |



**Table 9.** Results of the physical and chemical tests for the toxic characteristics of the solid residue intended for disposal: TCLP test.

| Parameter      | Unit | Found Value | Reference Value for Non-Hazardous Waste |
|----------------|------|-------------|---|
| Antimony, Sb   | mg/L | <0.011      | 15                                      |
| Barium, Ba     | mg/L | 0.09        | 100                                     |
| Chrome, Cr     | mg/L | <0.005      | 5                                       |
| Molybdenum, Mo | mg/L | <0.007      | 350                                     |
| Nickel, Ni     | mg/L | <0.036      | 20                                      |
| Selenium, Se   | mg/L | <0.033      | 1                                       |
| Zinc, Zn       | mg/L | 1.72        | 250                                     |
| Copper, Cu     | mg/L | <0.005      | 25                                      |
| Arsenic, As    | mg/L | <0.020      | 5                                       |
| Cadmium, Cd    | mg/L | 0.72        | 1                                       |
| Lead, Pb       | mg/L | <0.020      | 5                                       |
| Mercury, Hg    | mg/L | <0.0005     | 0.2                                     |
| Vanadium, V    | mg/L | <0.008      | 24                                      |
| Silver, Ag     | mg/L | <0.005      | 5                                       |

The results of the leachability test (LP test) showed that the waste was non-hazardous. The TCLP test showed that the waste had no toxic characteristics and could be disposed of in landfill as non-hazardous waste.

### 3.10. Treatment of the Solution After $PbCO_3$ Precipitation

After  $PbCO_3$  precipitation, the precipitation solution was adjusted to a concentration of 250 g/L of NaCl for reuse in  $PbSO_4$  leaching.

If the solution contained increased concentrations of impurities (Fe, Cu, Zn, Ag,  $SO_4^{2-}$ , etc.), it could be treated with NaOH solution until a pH of 10 was reached to precipitate residual silver in the form of  $Ag_2O$ . The  $Ag_2O$  precipitate can be further reduced with hydrazine and melted to obtain pure Ag.

The filtrate is chloride wastewater, which is then further purified at a chloride wastewater treatment plant.

### 3.11. Proposal for a Technological Scheme for the Treatment of Jarosite Pb–Ag Tailings

The proposed technological scheme for obtaining Cu, Zn, and Pb from jarosite waste, including a material balance, is shown in Figure 16.

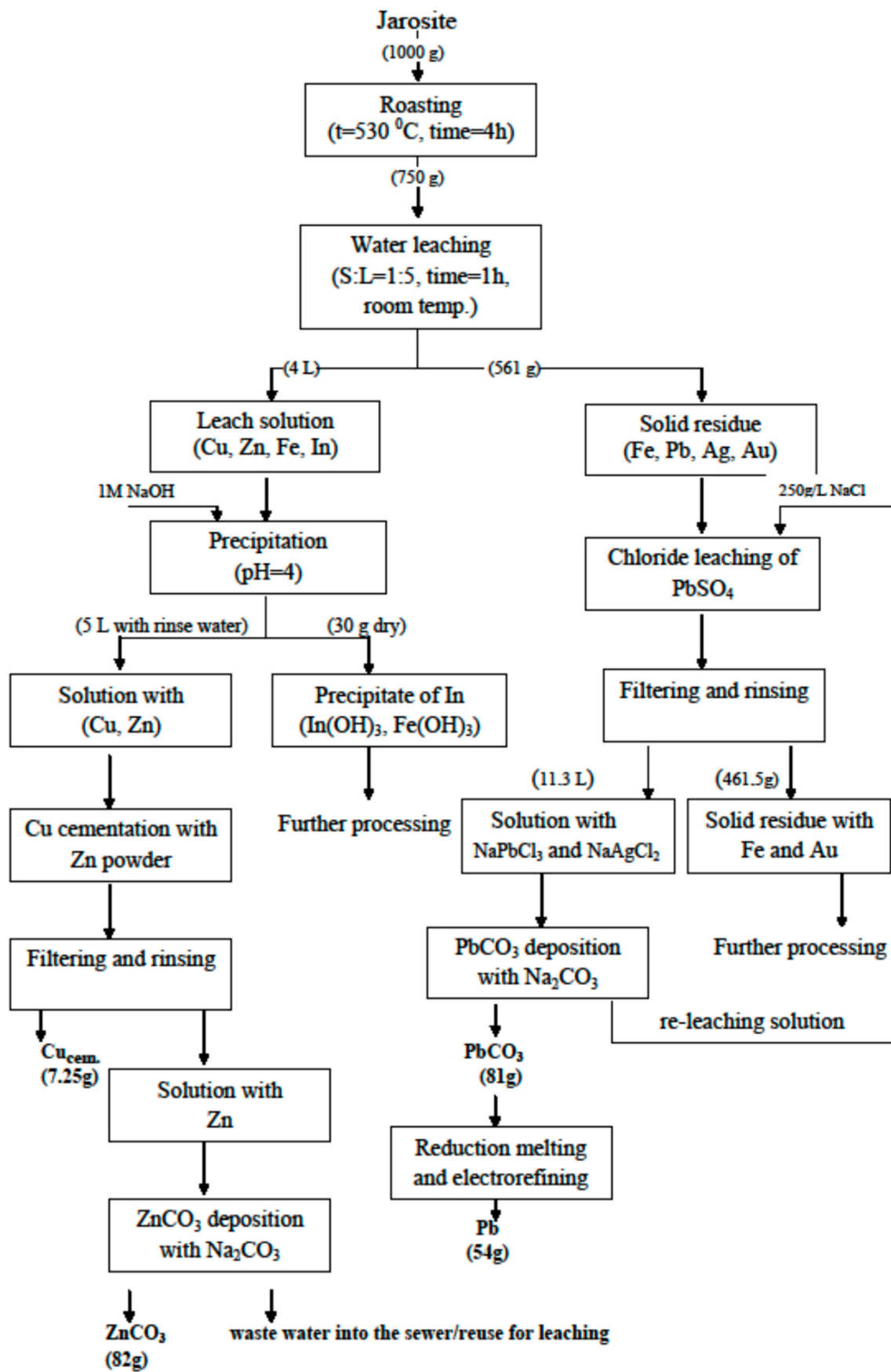


Figure 16. Technological scheme for obtaining Cu, Zn, and Pb from jarosite waste.

#### 4. Conclusions

Copper, zinc, lead, and silver from jarosite tailings waste were extracted through the following treatment phases: (I) the roasting of jarosite to convert ferric sulfate to water-insoluble hematite and (II) leaching Cu and Zn with water to obtain a  $\text{CuSO}_4 + \text{ZnSO}_4$  solution.

There was also insignificant dissolution of Fe because the following stages were conducted: (III) the precipitation of Fe from the leach solution with 1 M NaOH, (IV) the cementation of Cu with zinc from the  $\text{CuSO}_4 + \text{ZnSO}_4$  solution, (V) the precipitation of Zn from the  $\text{ZnSO}_4$  solution with  $\text{Na}_2\text{CO}_3$ , (VI) leaching of the solid residue obtained after water leaching with NaCl to dissolve Pb and its precipitation as  $\text{PbCO}_3$  with  $\text{Na}_2\text{CO}_3$ , and (VII)  $\text{PbCO}_3$  was further melted to obtain a Pb anode, which was then converted into a Pb cathode by electrolytic refining.

This work shows that the combination of roasting and leaching provides a promising process for obtaining Cu cement,  $\text{ZnCO}_3$ ,  $\text{PbCO}_3$ , and Pb in the form of commercial products.

The total recovery of Cu and Zn after roasting, leaching, Fe precipitation, cementation, and carbonate precipitation was 79.73% and 86.64%, respectively. The total recovery of Pb and Ag after chloride leaching was 96.05% and 87.5%, respectively. The technological scheme, along with the material balance, is presented in this paper.

The quality of the obtained products was as follows:

The composition of Cu cement was Cu = 75.97%, Zn = 7.31%, Fe = 0.005%, In < 0.095%, S = 1.9%, Ga < 0.002%, Ge < 0.002%, Ag = 0.042%, and Pb = 0.06%.

The composition of  $\text{ZnCO}_3$  was Zn = 52.22%, Cu = 0.26%, Fe = 0.84%, Pb = 0.002%, Ag < 0.001%, S = 2.24%, and In < 0.002%.

The composition of  $\text{PbCO}_3$  was Pb = 67.50%, Ag = 0.47%, Cu = 0.55%, Zn = 5.63%, Fe = 0.08%, S = 0.14%, and In < 0.06%.

Pb = 99.95%.

The obtained results were confirmed at an enlarged pilot level, after which the design of the plant was initiated by Elixir Company in Šabac, Serbia.

**Author Contributions:** Conceptualization, V.C.; methodology, V.C. and M.J.; investigation, D.S.B., Lj.A. and I.J.; writing—original draft preparation, V.C. and M.J.; writing—review and editing, D.M.B.; supervision, S.Đ. All authors have read and agreed to the published version of the manuscript.

**Funding:** The authors would like to thank Elixir Zorka, Serbia, for providing the sample and for their financial support in obtaining a solution to manage this waste (contract number 1061/19).

**Data Availability Statement:** Data are contained within this article.

**Acknowledgments:** This work was supported by the Ministry of Science, Technological Development, and Innovation of the Republic of Serbia under the contract on realization, and the financing of scientific research by the Mining and Metallurgy Institute Bor in 2024 (contract number: 451-03-66/2024-03/200052).

**Conflicts of Interest:** The authors declare no conflicts of interest.

#### References

1. Koppelaar, R.H.E.M.; Koppelaar, H. The Ore Grade and Depth Influence on Copper Energy Inputs. *Biophys. Econ. Resour. Qual.* **2016**, *1*, 11. [CrossRef]
2. González-Ibarra, A.A.; Nava-Alonso, F.; Fuentes-Aceituno, J.C.; Uribe-Salas, A. Hydrothermal decomposition of industrial jarosite in alkaline media: The rate determining step of the process kinetics. *J. Min. Metall. Sect. B-Metall.* **2016**, *52*, 135–142. [CrossRef]
3. Konieczny, A.; Pawlos, W.; Malgorzata, K. Evaluation of organic carbon separation from copper ore by pre-flotation. *Physicochem. Probl. Miner. Process.* **2013**, *49*, 189–201.
4. Nayak, A.; Jena, M.S. Mineralogical characterization for selection of possible beneficiation route for low grade lead-zinc ore of Rampura Agucha, India. *Trans. Indian Inst. Met.* **2020**, *73*, 775–784. [CrossRef]
5. Yin, J.; Zhang, W.; Sun, G.; Xiao, S.; Lin, H. Oxygen-functionalized defect engineering of carbon additives enable lead-carbon batteries with high cycling stability. *J. Energy Storage* **2021**, *43*, 103205. [CrossRef]

6. Erdem, M.; Yurten, M. Kinetics of Pb and Zn leaching from zinc plant residue by sodium hydroxide. *J. Min. Metall. Sect. B Metall.* **2015**, *51*, 89–95. [[CrossRef](#)]
7. Turan, M.D.; Altundogan, H.S.; Tümen, F. Recovery of zinc and lead from zinc plant residue. *Hydrometallurgy* **2004**, *75*, 169–176. [[CrossRef](#)]
8. Nayak, A.; Jena, M.S.; Mandre, N.R. Beneficiation of Lead-Zinc ores—A review. *Min. Proc. Ext. Met. Rev.* **2022**, *43*, 564–583. [[CrossRef](#)]
9. Rahman, M.L.; Sarjadi, M.S.; Guerin, S.; Sarkar, S.M. Poly(amidoxime) Resins for Efficient and Eco-friendly Metal Extraction. *ACS Appl. Polym. Mater.* **2022**, *4*, 2216–2232. [[CrossRef](#)]
10. Sunder, G.S.S.; Rohanifar, A.; Alipourasiabi, N.; Lawrence, J.G.; Kirchoff, J.R. Synthesis and Characterization of Poly(pyrrole-1-carboxylic acid) for Preconcentration and Determination of Rare Earth Elements and Heavy Metals in Water Matrices. *ACS Appl. Mater. Interfaces* **2021**, *13*, 34782–34792. [[CrossRef](#)]
11. Chu, F.X.; Liu, C.; Wu, H.; Liu, X. Advances in Chelating Resins for Adsorption of Heavy Metal Ions. *Ind. Eng. Chem. Res.* **2022**, *61*, 11309–11328. [[CrossRef](#)]
12. Chen, T.; Li, H.; Wang, H.; Zou, X.; Liu, H.; Chen, D.; Zhou, Y. Removal of Pb(II) from Aqueous Solutions by Periclase/Calcite Nanocomposites. *Water. Air Soil Pollut.* **2019**, *230*, 299–314. [[CrossRef](#)]
13. Lalmi, A.; Bouhidel, K.-E.; Sahraoui, B.; Anfif, C.E.H. Removal of lead from polluted waters using ion exchange resin with Ca(NO<sub>3</sub>)<sub>2</sub> for elution. *Hydrometallurgy* **2018**, *178*, 287–293. [[CrossRef](#)]
14. Wang, N.; Bora, M.; Song, H.; Tao, K.; Wu, J.; Hu, L.; Liao, J.; Lin, S.; Triantafyllou, M.S.; Li, X. Hyaluronic Acid Methacrylate Hydrogel-Modified Electrochemical Device for Adsorptive Removal of Lead(II). *Biosensors* **2022**, *12*, 714. [[CrossRef](#)]
15. Ren, H.; Li, B.; Neckenig, M.; Wu, D.; Li, Y.; Ma, Y.; Li, X.; Zhang, N. Efficient lead ion removal from water by a novel chitosan gel-based sorbent modified with glutamic acid ionic liquid. *Carbohydr. Polym.* **2019**, *207*, 737–746. [[CrossRef](#)] [[PubMed](#)]
16. Sahoo, P.K.; Das, S.C. Recovery of lead from zinc plant waste. *Trans. Indian Inst. Met.* **1986**, *39*, 604–608.
17. Vinals, J.; Nunez, C.; Carasco, J. Leaching of gold, silver and lead from plumbojarosite-containing hematite tailings in HCl-CaCl<sub>2</sub> media. *Hydrometallurgy* **1991**, *26*, 179–199. [[CrossRef](#)]
18. Kunda, W.; Veltman, H. Decomposition of jarosite. *Metall. Trans.* **1979**, *10*, 439–446. [[CrossRef](#)]
19. Božić, D.; Conić, V.; Dragulović, S.; Avramović, L.; Jonović, R.; Bugarin, M. Laboratorijska istraživanja luženja Cu, Zn i In iz otpadnog taloga jarozita. *Ecologica* **2021**, *28*, 481–486. [[CrossRef](#)]
20. Abidli, A.; Huang, Y.; Rejeb, Z.B.; Zaoui, A.; Park, C.B. Sustainable and efficient technologies for removal and recovery of toxic and valuable metals from wastewater: Recent progress, challenges, and future perspectives. *Chemosphere* **2022**, *292*, 133102.
21. Xolo, L.; Boyce, P.M.; Makelane, H.; Faleni, N.; Tshentu, Z.R. Status of Recovery of Strategic Metals from Spent Secondary Products. *Minerals* **2021**, *11*, 673. [[CrossRef](#)]
22. Dutrizac, J.E.; Dinardo, O. The co-precipitation of copper and zinc with lead jarosite. *Hydrometallurgy* **1983**, *11*, 61–78. [[CrossRef](#)]
23. Cruells, M.; Roca, A.; Patiño, F.; Salinas, E.; Rivera, I. Cyanidation kinetics of argentian jarosite in alkaline media. *Hydrometallurgy* **2000**, *55*, 153–163. [[CrossRef](#)]
24. Patiño, F.; Reyes, I.A.; Flores, M.U.; Pandiyan, T.; Roca, A.; Reyes, M.; Hernández, J. Kinetic modeling and experimental design of the sodium arsenojarosite decomposition in alkaline media: Implications. *Hydrometallurgy* **2013**, *137*, 115–125. [[CrossRef](#)]
25. Hudson-Edwards, K.A. Uptake and release of arsenic and antimony in alunite-jarosite and beudantite group minerals. *Am. Min.* **2012**, *334*, 9–24. [[CrossRef](#)]
26. Flores, V.H.; Patiño, F.; Roca, A.; Flores, M.U.; Reyes, I.A.; Reyes, M.; Islas, H. Alkaline Decomposition of Solid Solution of Ammonium-Sodium Jarosite with Arsenic. *Metals* **2022**, *12*, 584. [[CrossRef](#)]
27. Frost, R.L.; Weier, M.L.; Martens, W. Thermal decomposition of jarosites of potassium, sodium and lead. *J. Therm. Anal. Calorim.* **2005**, *82*, 115–118. [[CrossRef](#)]
28. Conić, V.; Božić, D.; Dragulović, S.; Avramović, L.J.; Jonović, R.; Bugarin, M. Research on acid leaching of Cu, Zn and in from Jarosite waste. In Proceedings of the XIV International Mineral Processing and Recycling Conference, Belgrade, Serbia, 12–14 May 2021.
29. Janošević, M.; Conić, V.; Božić, D.; Avramović, L.; Jovanović, I.; Kamberović, Ž.; Marjanović, S. Indium Recovery from Jarosite Pb–Ag Tailings Waste (Part 1). *Minerals* **2023**, *13*, 540. [[CrossRef](#)]
30. Conić, V.T.; Pešovski, B.D.; Cvetkovski, V.B.; Stanojević-Šimšić, Z.S.; Dragulović, S.S.; Simonović, D.B.; Dimitrijević, S.B. Lead sulphate leaching by sodium chloride solution. *Chem. Ind.* **2013**, *67*, 485–494. [[CrossRef](#)]

**Disclaimer/Publisher’s Note:** The statements, opinions and data contained in all publications are solely those of the individual author(s) and contributor(s) and not of MDPI and/or the editor(s). MDPI and/or the editor(s) disclaim responsibility for any injury to people or property resulting from any ideas, methods, instructions or products referred to in the content.